Available online at www.sciencedirect.com
ScienceDirect
Polymer 48 (2007) 3520–3529
polymer
www.elsevier.com/locate/polymer

Effect of microcapsule size on the performance of self-healing polymers

Joseph D. Rule [a,1], Nancy R. Sottos [b], Scott R. White [a,*]

[a] Department of Aerospace Engineering and Beckman Institute, University of Illinois, 405 North Mathews Avenue, Urbana, IL 61801, United States
[b] Department of Materials Science and Engineering and Beckman Institute, University of Illinois, 405 North Mathews Avenue, Urbana, IL 61801, United States

Received 1 November 2006; received in revised form 29 March 2007; accepted 1 April 2007
Available online 12 April 2007

Abstract

The influence of microcapsule diameter and crack size on the performance of self-healing materials is investigated. These epoxy-based materials contain embedded Grubbs' catalyst particles and microencapsulated dicyclopentadiene (DCPD). Autonomic repair is triggered by rupture of the microcapsules in response to damage, followed by release of DCPD into the crack plane where it mixes with the catalyst and polymerizes. The amount of liquid that microcapsules deliver to a crack face is shown to scale linearly with microcapsule diameter for a given weight fraction of capsules. In addition, self-healing performance reaches maximum levels only when sufficient healing agent is available to entirely fill the crack. Based on these relationships, the size and weight fraction of microcapsules can be rationally chosen to give optimal healing of a predetermined crack size. By using this strategy, self-healing is demonstrated with smaller microcapsules and with lower weight fractions of microcapsules than have been possible in previous self-healing systems.

Keywords: Autonomic materials; Self-healing; Fracture

1. Introduction

Major advances have been made in the past decade within the field of ''smart'' polymeric materials, such as shape-memory polymers [1] or adaptive and responsive polymer surfaces [2]. The common theme among these materials is that they respond autonomically to specific stimuli using in situ functionality. Self-healing polymers are another recently developed class of smart materials where the objective is complete, passive repair of minor damage without the need for detection or any type of manual intervention [3–7]. Damage to the material acts as the stimulus, and the response is a process that autonomically repairs that damage.

While several general self-healing strategies have been investigated, one of the most successful and versatile approaches utilizes embedded microcapsules that are filled with a liquid healing agent [3,8–14]. When a crack propagates through the material, it ruptures the microcapsules and releases the healing agent into the damaged area. In the crack plane, the healing agent is exposed to catalyst that has been separately dispersed in the material. The catalyst causes polymerization of the healing agent, thus repairing the damage autonomically. Self-healing via microencapsulation has been used to repair different thermosetting polymeric materials both in their neat form [3,8,11,12] and in fiber-reinforced composites [10], and multiple healing agent/catalyst chemistries are viable [12,15]. The chemical system that has been studied most extensively in self-healing materials consists of microencapsulated DCPD that is polymerized by Grubbs' catalyst through ring-opening metathesis polymerization (ROMP). This specific chemical system is examined herein.

* Corresponding author. Tel.: +1 217 333 1077; fax: +1 217 244 0181.
E-mail address: swhite@uiuc.edu (S.R. White).
[1] Present address: 3M Corporate Research Laboratory, 3M Center Building 0201-03-N-04, St. Paul, MN 55144-1000, United States.

0032-3861/$ - see front matter © 2007 Elsevier Ltd. All rights reserved.
doi:10.1016/j.polymer.2007.04.008

In prior self-healing studies [3,8,11,12], the microcapsules containing healing agent have been on the size scale of ~100 μm. While this size regime is appropriate for some potential applications, there is significant technological interest in reducing the size of the microcapsules. Smaller microcapsules are necessary when one of the characteristic dimensions of a material is smaller than 100 μm (e.g. thin coatings or interstices in high fiber volume fraction composites). Moreover, self-healing requires that both a microcapsule and a catalyst particle are intersected by the same crack path or network. Isolated microcracks in a material that are similar in size to the microcapsules are unlikely to contact both components of the self-healing system, and therefore will not be repaired. Reducing the size of the microcapsules may enable self-healing of smaller forms of damage like microcracks.

Procedures for making smaller microcapsules (<10 μm) have been reported in the literature [16–20], so self-healing materials with smaller components can be synthesized. However, we have previously observed that when small microcapsules are used, they must be included in higher weight fractions to achieve efficient self-healing [11]. The aim of this paper is to systematically investigate both theoretically and empirically how the size of the microcapsules affects self-healing performance. Understanding this fundamental relationship is critical for the rational design of self-healing materials.

2. Experimental section

EPON 828 was purchased from Miller-Stephenson (Morton Grove, Illinois) and diethylenetriamine (DETA) was obtained from Air Products (Allentown, Pennsylvania). Bis(tricyclohexylphosphine)benzylidene ruthenium (IV) dichloride (first generation Grubbs' catalyst) [21] was obtained from Sigma–Aldrich (Saint Louis, Missouri) and recrystallized by either freeze-drying or non-solvent addition as reported elsewhere [22]. *endo*-DCPD was purchased from Acros (Morris Plains, New Jersey) and distilled before use, and 150 ppm *tert*-butylcatechol was added as an inhibitor. Poly(vinyl alcohol) was purchased from Sigma–Aldrich (Saint Louis, Missouri) and had a typical M_w of 85,000–124,000 and was 87–89% hydrolyzed. Paraffin wax was obtained from Sigma–Aldrich (Saint Louis, Missouri) and had a melting range of 58–62 °C.

DCPD was microencapsulated using the previously described procedure [3,9]. Microcapsules were produced with volume-weighted average diameters of 14(6), 29(10), 63(15), 151(17), 251(31), and 386(48) μm by using stirring rates of 2400, 1600, 1000, 450, 350, and 200 rpm, respectively. The values in parentheses represent the standard deviations of the distribution of microcapsule diameters.

In all cases, the Grubbs' catalyst was delivered within wax microspheres [12]. In some specifically indicated cases, the catalyst had been recrystallized by non-solvent addition, but otherwise, the catalyst used had been recrystallized through freeze-drying before being cast into the wax [22]. To make the wax microspheres, the catalyst (1.0 g) was heated in a 20 mL vial with paraffin wax (9.0 g) until the wax had melted, and this mixture was then poured into a hot aqueous solution of poly(vinyl alcohol) (200 mL, 0.25 wt%, 70 °C) stirred at 800 rpm with a mechanical mixer. After stirring for 120 s, cold water (600 mL, 0 °C) was rapidly added. The resulting wax microspheres containing suspended Grubbs' catalyst were removed by filtration and dried under vacuum. The average diameter was 220 μm with a standard deviation of 110 μm. In all of our self-healing specimens, 5 wt% of these microspheres were included.

As in our previous work [8], fracture samples were prepared with a TDCB geometry using EPON 828 cured with 12 parts DETA per 100 parts of resin. However, the specimens in this work differ from those used previously in that catalyst was included only in the center section (7 mm wide) near the centerline groove (see Appendix). In the cases where DCPD microcapsules were included in the center section, DCPD microcapsules were also included in the outer section (10 wt%, average diameter = 180 μm). The specimens were cured for 24 h at room temperature and for an additional 24 h at 35 °C. The density of the specimens was approximately 1.16 g/cm^3.

Fracture tests followed the established procedure [3,8,11,12] in which a razor blade was used to initiate a pre-crack. Tape was applied to the base of the specimens (farthest from the pin-loading holes) to prevent the two halves of the specimen from violently separating when the crack propagated through the entire specimen. The specimens were then pin loaded and tested under displacement control at a rate of 5 μm/s. Specimens with a 47 mm molded groove were completely fractured, and the two halves were then brought back into contact and left to heal for 24 h at room temperature before retesting to failure. The fracture planes of all the 47 mm groove samples had essentially the same area, so the self-healing performance was quantified by the strain energy-to-failure (or internal work) for each healed specimen as given by the area under the load–displacement curve [12]. The peak load achieved during fracture of the self-healed test specimens was also used to quantify healing performance.

TDCB specimens with a short groove (which were used to produce less crack face separation) were also produced, and are similar to the localized TDCB described above, but the groove is shortened from 47 mm to 25 mm (Fig. 1). In addition, the center section which contains the catalyst has a total length of 64 mm rather than 86 mm. In all other dimensions, they are identical to the TDCB specimens used in our previous self-healing trials. Specimens with a 25 mm molded groove were fractured only to the end of the groove and were then unloaded and left to heal similarly. In all plots, each data point represents the average of between four and six trials, and the error bars are +/−1 standard deviation.

3. Microcapsule size and healing agent delivery

Consider a self-healing polymer containing microcapsules of a healing agent dispersed randomly as shown in Fig. 2. If a planar crack propagates through this material system, then all microcapsules that are intersected by the plane will rupture

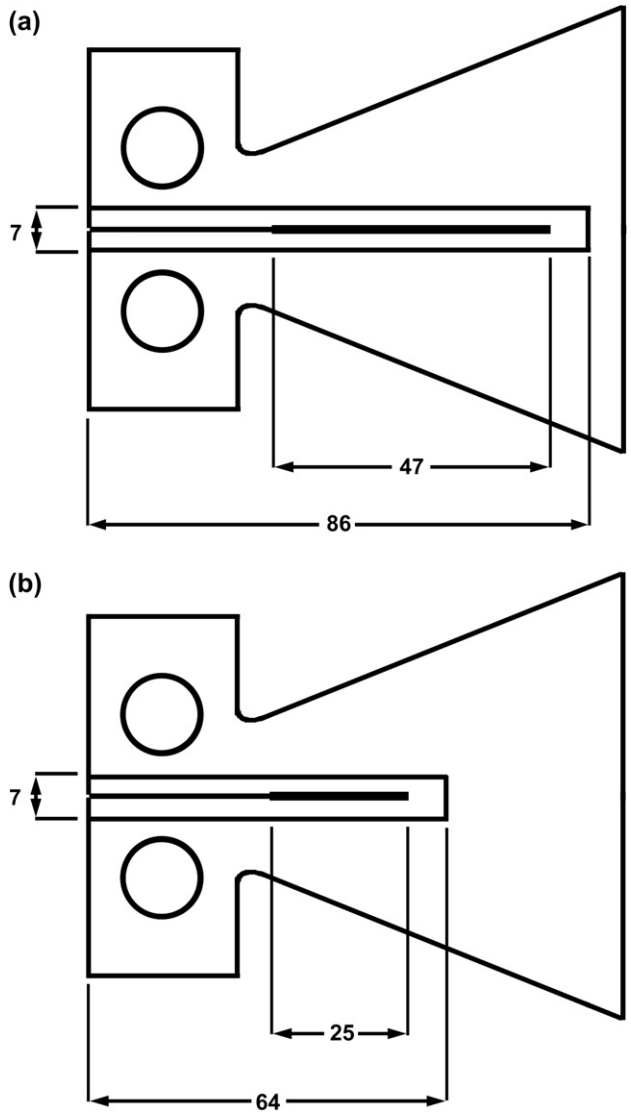

Fig. 1. Dimensions of localized TDCB fracture specimens with (a) a 47 mm groove and (b) a 25 mm groove.

and release their contents. The number of capsules that are ruptured (n) is simply,

$$n = pN \tag{1}$$

where N is the total number of capsules in the sample and p is the probability that the center of a capsule lies within the rupture zone of the crack plane (equal to one microcapsule diameter). Assuming that the capsules are randomly distributed and that the capsule shell is negligible (<2% of the capsule diameter), the probability should be,

$$p = \frac{\rho_s A d_c}{M_s} \tag{2}$$

where ρ_s is the density of the sample, A is the crack area, d_c is the diameter of the capsules, and M_s is the total mass of the sample. The numerator in Eq. (2) simply represents the mass of material within the rupture zone. In addition, the total

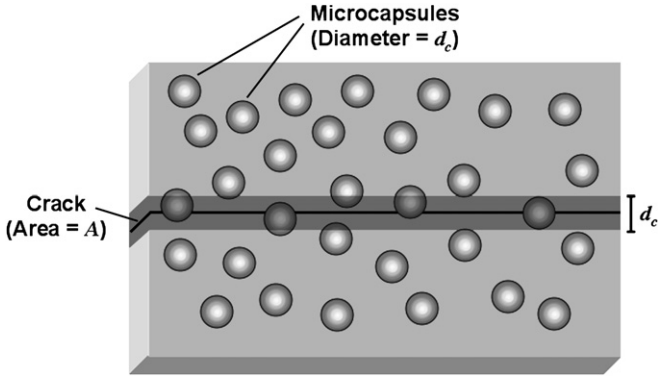

Fig. 2. Schematic of microcapsules within an epoxy matrix. Any microcapsules with centers lying inside the shaded region are intersected (and presumably ruptured) by the crack.

number of capsules in the sample can be calculated based on the microcapsule weight fraction,

$$N = \frac{\Phi M_s}{m_c} \tag{3}$$

where Φ is the mass fraction of microcapsules and m_c is the mass of each microcapsule.

The amount of delivered healing agent normalized by crack area ($\overline{m}$) is simply,

$$\overline{m} = \frac{m_h}{A} = \frac{n m_c}{A} \tag{4}$$

where m_h is the total mass of healing agent delivered assuming all microcapsules intersected by the crack plane are ruptured. Combining Eqs. (1)–(4) yields,

$$\overline{m} = \rho_s \Phi d_c \tag{5}$$

Thus, the total mass of healing agent available for delivery per unit crack area is proportional to both microcapsule weight fraction and diameter.

4. Results and discussion

4.1. Effect of component size

The relationship between microcapsule size, healing agent delivery and healing performance was further investigated through fracture testing. TDCB specimens were prepared using microcapsules with weight-average diameters of 63 μm, 151 μm, and 386 μm at various weight fractions. The specimens were fractured, and the two halves were brought back into contact and allowed to self-heal for 24 h before testing the healing performance. Both the average strain energy-to-failure and the average peak load borne by the self-healed specimens are presented in Fig. 3 for each microcapsule size and weight fraction. In terms of energy and peak load, specimens with larger capsules perform better than those with smaller capsules at the same weight fraction.

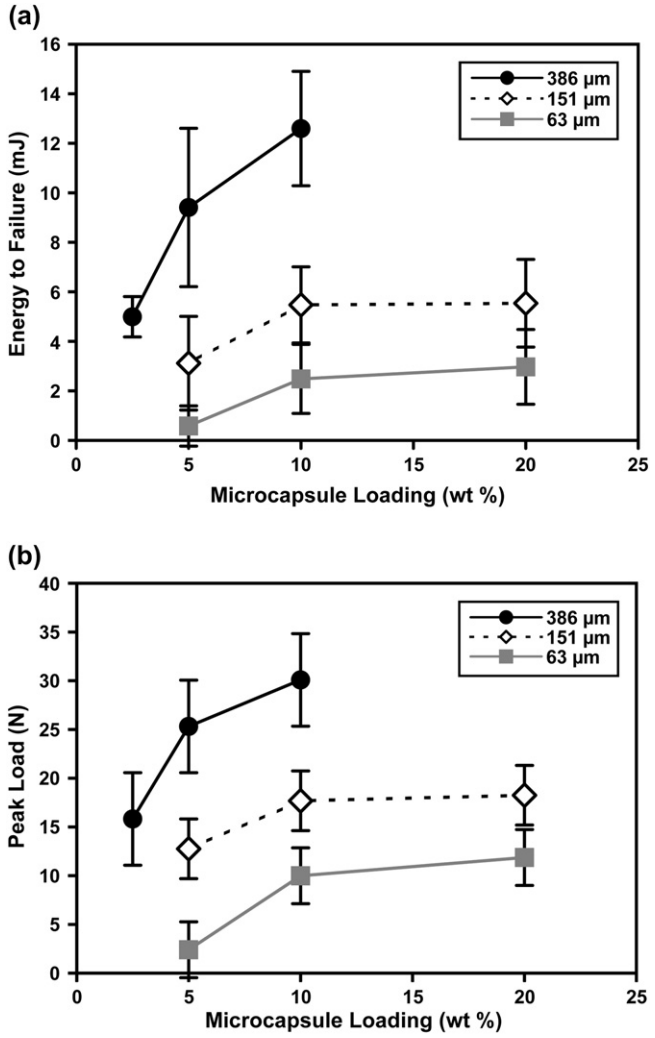

Fig. 3. Fracture test results in terms of both (a) strain energy-to-failure and (b) peak load for self-healed TDCB specimens with varying microcapsule sizes and weight fractions.

While Fig. 3 shows the self-healing performance as a function of microcapsule weight fraction, Fig. 4 shows the healing performance (for the same set of experiments) as a function of the theoretical amount of available healing agent per unit crack area as calculated by Eq. (5). In this case, the *x*-axis value is determined by the product of the microcapsule size and the microcapsule weight fraction. The figure also shows data for experiments where the DCPD healing agent was delivered by manual injection instead of by microcapsules (vide infra). Compared to Fig. 3, the data in Fig. 4 are grouped together more strongly, especially when the microcapsule weight fraction is less than 20 wt%. These results suggest that the observed healing performance in this system is largely coupled to the product of microcapsule size and microcapsule weight fraction. Assuming that self-healing performance depends on the amount of available healing agent, these data support the validity of Eq. (5). The exception is when high weight fractions (20%) of healing agent are used. The relatively lower performance observed with 20 wt% microcapsules was repeatable over a large number of samples, but the exact reason for the deviation is not clear.

The average volume of the crack in the fractured TDCB specimens was examined by light microscopy to determine how the amount of required healing agent relates to the volume of the crack that is being repaired. The average crack face separation is 26 μm (standard deviation = 7 μm) near the top of the fractured sample (i.e. closest to the pin-loading holes, Fig. 5a) and 8 μm (standard deviation = 3 μm) near the bottom of the sample. With a crack face separation of 26 μm, the crack volume is 2.6 μL/cm^2 of crack area. Thus, it would be expected that a healing agent delivery of at least 2.6 mg/cm^2 would be needed to completely fill this crack and give maximum self-healing (density of DCPD = 0.98 g/cm^3). Not surprisingly, Fig. 4 shows that healing performance declines rapidly when healing agent delivery is less than 2.6 mg/cm^2.

The experimental data in Fig. 3 demonstrate that at a given weight fraction, larger microcapsules produce superior healing performance, and theory suggests that this increased performance is due to the delivery of more healing agent per unit crack area. SEM images of fracture surfaces further confirm that the increase in healing performance from the larger capsules is due to delivery of greater amounts of healing agent. Fig. 6a shows a representative crack plane from a specimen with 20 wt% of 63 μm microcapsules after being fractured, healed, and fractured again. Patches of polymerized DCPD are present on the fracture surface, but the coverage is incomplete. Fig. 6b is an analogous image from a specimen with 10 wt% of 386 μm microcapsules. Despite having a lower weight fraction of microcapsules present, the coverage of polymerized DCPD is now nearly complete over the entire crack plane.

The data in Figs. 3 and 4 indicate that the product of microcapsule size and weight fraction controls both the amount of healing agent available in the crack plane and the level of self-healing that is achieved. However, these data alone cannot confirm that the calculated amounts of healing agent delivery are quantitatively accurate. Therefore, further tests were performed with TDCB specimens containing catalyst, but not DCPD microcapsules. These specimens were fractured and then measured amounts of healing agent were manually delivered to the crack plane using a syringe. The two halves of each fractured specimen were then rejoined and held in contact for 24 h before retesting. These experiments are analogous to the self-healing tests, but they differ in that the amount of healing agent on the crack plane is explicitly known and is manually applied.

The results of the tests with manually injected healing agent are shown in Fig. 4 together with the data from self-healing specimens in which the healing agent is delivered autonomically via microcapsules. The data for the manually injected healing agent follow nearly the same trend as the data in which microcapsules are used for healing agent delivery. The agreement of these results indicates that the calculations of healing agent delivery using Eq. (5) are reasonably accurate.

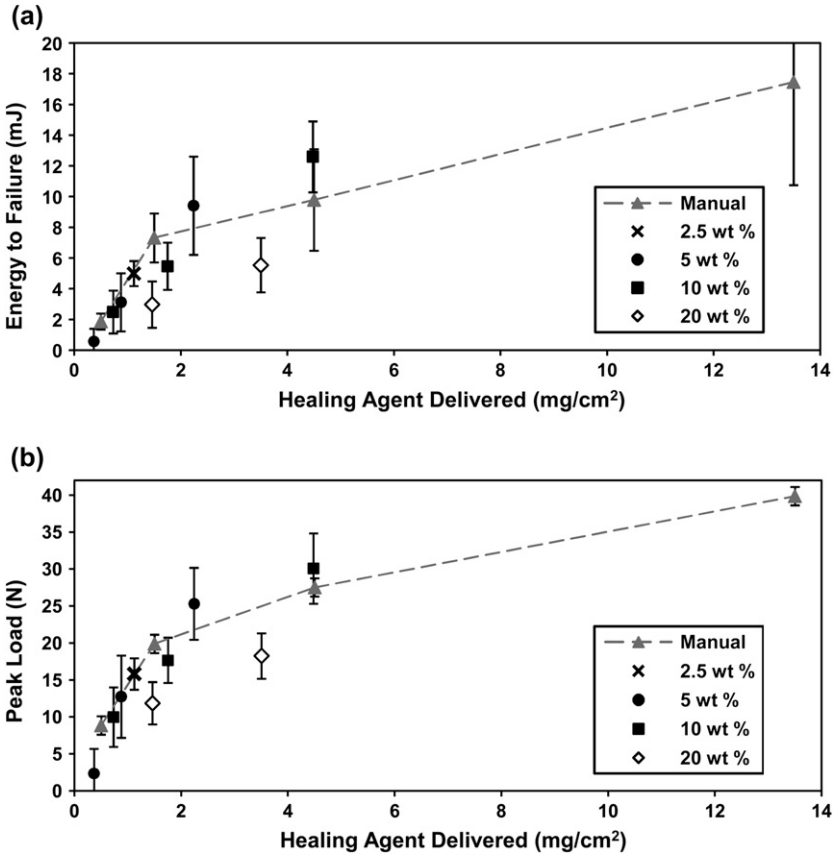

Fig. 4. Fracture test results of self-healed TDCB specimens as a function of healing agent delivery as calculated by Eq. (5).

The data in Fig. 4 also suggest that the amount of healing agent that was delivered autonomically using microcapsules was too low to reach the full potential healing performance. The best healing achieved using microcapsules resulted from specimens containing 10 wt% of 386 μm microcapsules, which corresponds to about 4.5 mg of healing agent delivered per unit crack area. An increase of about 40% in strain energy-to-failure and roughly 30% in peak load was achieved through manual injection of 13.5 mg/cm^2 healing agent onto the fracture plane. Thus, improved self-healing performance could be achieved by delivering more healing agent to the crack plane, which theoretically can be accomplished by higher weight fractions of microcapsules. However, based on the crack volume measurements, 4.5 mg/cm^2 is sufficient healing agent to fill the crack, and a more efficient use of the available healing agent could yield better performance. For example, increasing the catalyst concentration accelerates polymerization and could reduce the time for evaporation or absorption of the DCPD, thus reducing the amount of healing agent required.

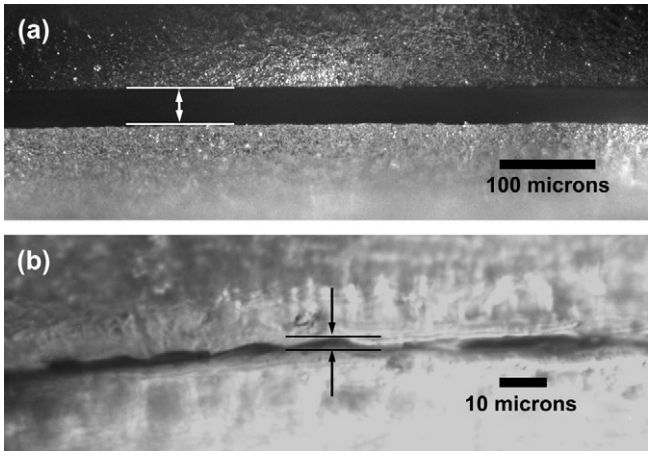

Fig. 5. Light microscopic images of a crack under autonomic repair in (a) a fully fractured specimen with a 47 mm groove and (b) a specimen with a 25 mm groove which is only fractured to the end of that groove. Both images are of the widest part of the crack nearest the pin-loading holes. Arrows indicate crack width measurements.

In this study, catalyst delivery was improved by altering the catalyst crystal morphology. In the experiments presented in Fig. 4, the catalyst was recrystallized through freeze-drying and then encapsulated in wax microspheres. This freeze-dried catalyst is made up of small crystals (<1 μm) fused together in porous sheets of about 1 μm thick [22]. Although protected by the wax, the small crystal morphology with high surface area that results from freeze-drying is more easily deactivated by the curing agent for the epoxy resin compared to other large catalyst morphologies [22]. This deactivation results in slower polymerization since the amount of active catalyst is reduced. Larger catalyst crystals with different morphology were obtained through a recrystallization procedure using non-solvent addition [22]. The resulting crystals are rodlike with a diameter

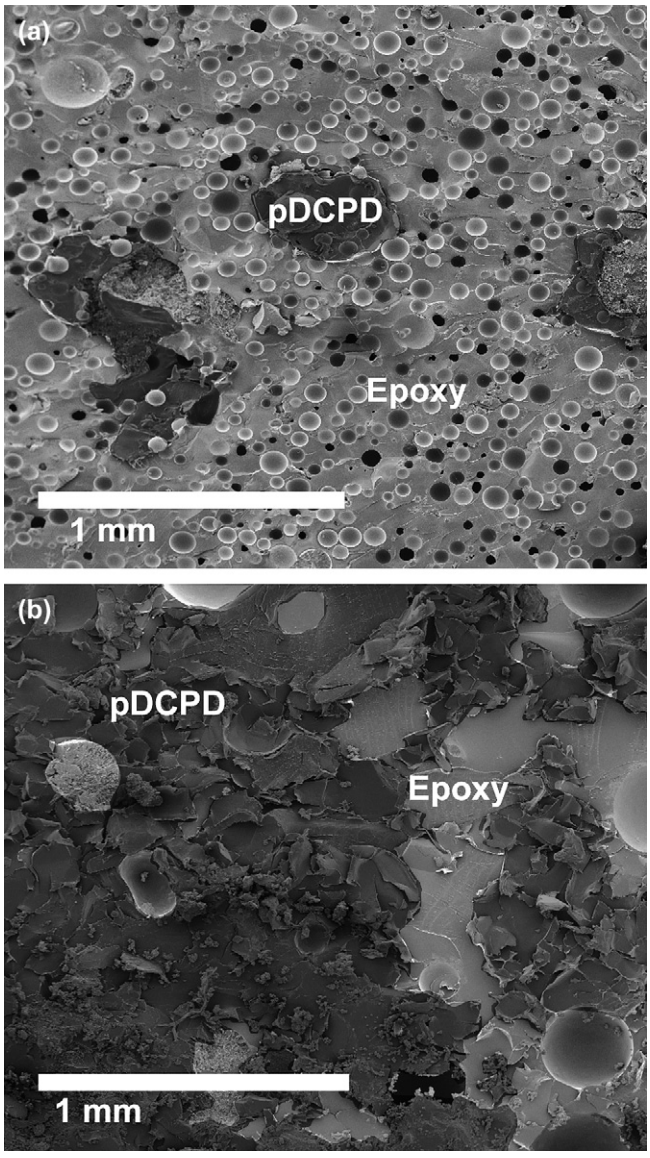

Fig. 6. Fracture planes after self-healing of specimens containing (a) 20 wt% of microcapsules with an average diameter of 63 μm or (b) 10 wt% or microcapsules with an average diameter of 386 μm. The polyDCPD has been darkened to enhance contrast.

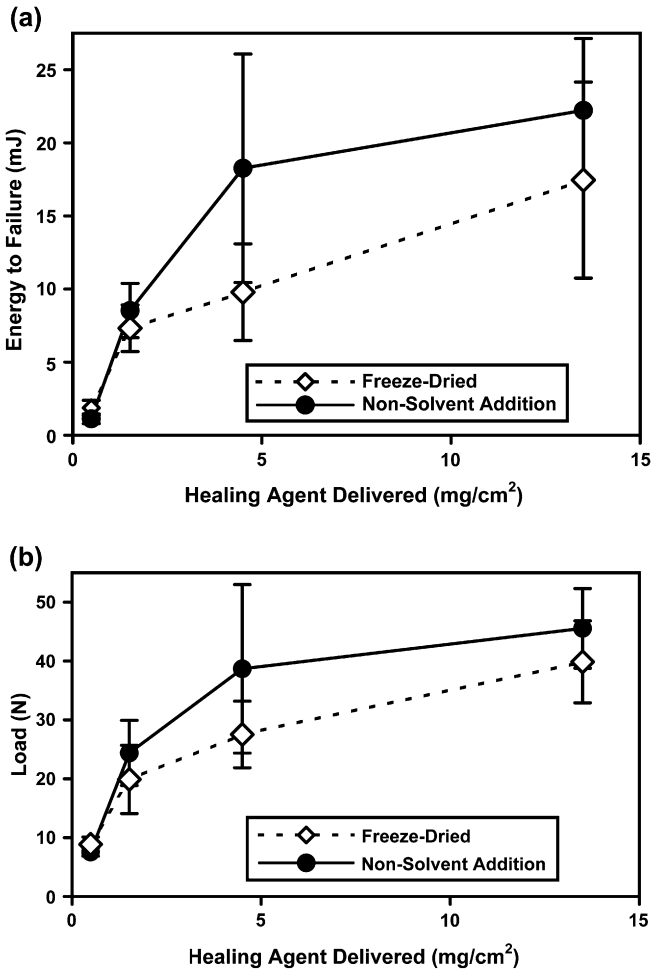

Fig. 7. Influence of the catalyst crystal morphology on healing performance with manually applied DCPD. The catalyst used in the specimens had been recrystallized through either non-solvent addition or freeze-drying.

of about 2 μm and lengths of more than 10 μm, and they possess a good blend of fast dissolution and less deactivation [22]. The effect of catalyst crystal morphology on healing performance is summarized in Fig. 7. It is important to note that while the size and morphology of the catalyst crystals vary, the wax microspheres in which these crystals are embedded are all of approximately the same average size. Therefore, the catalyst-bearing microspheres in all experiments have a similar level of dispersion in the epoxy matrix in spite of the fact that the catalyst crystals embedded in these microspheres may be different. The larger crystal morphology associated with non-solvent addition significantly improved the healing performance. Greater energy-to-failure and peak loads were achieved using less healing agent than for the freeze-dried catalyst morphology. Hence, healing performance can be enhanced through more efficient delivery of catalyst and efficient use of available healing agent.

4.2. Effect of crack size

Since self-healing performance is impacted by delivery of sufficient healing agent for the crack volume to be repaired, smaller crack volumes should exhibit reduced requirements of healing agent delivery. To test this hypothesis, a modified fracture specimen was designed. All previous experiments were performed with cracks that propagated all the way to the end of the TDCB specimens. The two halves of the specimen were clamped back together after initial fracture in a way that does not exert any force to press the crack faces back together, but only places the two halves in contact. This procedure results in an average crack face separation of about 26 μm near the loading pin holes of the sample. A modified TDCB sample incorporates a crack-directing groove that is reduced from 47 mm long to 25 mm long (Fig. 1). As a result, when the specimen is initially fractured, the virgin crack propagates only until it reaches the end of the groove. The sample is then unloaded and set aside to allow self-healing to occur.

The unfractured material in front of the crack tip reduces the crack face separation by both ensuring alignment of the two crack faces and preventing complete separation of the crack planes. Average crack face separation of these specimens is reduced to about 3 μm near the loading pin holes (Fig. 5b) and gradually decreases moving towards the crack tip.

In the fracture tests using the short groove, the virgin fracture is comparable to the standard TDCB specimen and the peak load occurs right before the crack propagates. However, the healed fracture tests with the short-groove specimen are complicated by the load that is borne by the unfractured material ahead of the groove. Sample compliance was used to clearly distinguish the contribution of self-healing in these tests. Fig. 8a shows the response for a non-self-healing control case containing microcapsules but not catalyst. The virgin load–displacement curve shows the expected drop in load as the crack initially propagates to the end of the groove and a new sample compliance is then established. After unloading and resting for 24 h, this control sample was loaded again and exhibits linear elastic behavior with the same compliance that was established at the end of the virgin fracture test.

In the case where self-healing does occur, the healed load–displacement curve is noticeably different (Fig. 8b). The compliance is initially the same as the virgin fracture test and this indicates that the crack has healed. As the load increases, the crack propagates and the sample compliance is dramatically increased as the healed crack reopens. Subsequently, the unfractured material ahead of the groove begins to bear load and linear elastic bending is again established at this increased compliance. The peak healed load is defined as the highest load achieved by the sample before the sample compliance increases.

Since the crack faces with these short-groove specimens are much less separated compared to the long-groove specimens (Fig. 5), the corresponding crack volume is also greatly reduced. Smaller crack volumes associated with the short-groove specimens should require less healing agent for successful self-healing. Fracture tests were performed to confirm this hypothesis. A series of test specimens with the short groove were prepared using various weight fractions of microcapsules with an average diameter of 251 μm. A corresponding control series with long-groove specimens were also prepared using the same set of microcapsules. Wax microspheres with catalyst crystals obtained using the non-solvent addition technique were used in both series of tests. The fracture test results (Fig. 9) show that the short-groove specimens produce excellent healing with microcapsule weight fractions as low as 1.25 wt% while the performance of the long-groove specimens decreases when the weight fraction drops below 10 wt%. This result confirms that smaller crack volumes require less healing agent delivery to achieve maximum self-healing. This result is also significant because it represents the lowest weight fraction of microcapsules to date in an effective self-healing test.

Since the healing agent available to the crack plane is linearly related to the diameter of the microcapsules (Eq. (5))

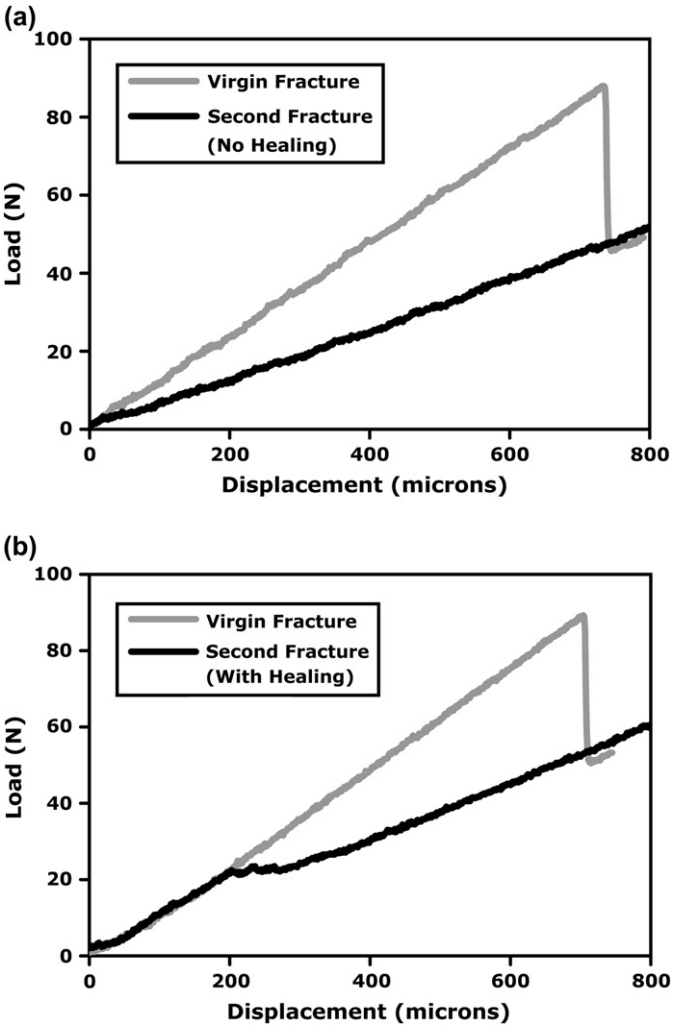

Fig. 8. Representative load–displacement curves for fracture tests of short-groove TDCB specimens with (a) 10 wt% microcapsules (251 μm), but no catalyst (and no self-healing ability) and (b) 2.5 wt% microcapsules (251 μm) with 5 wt% catalyst and successful self-healing.

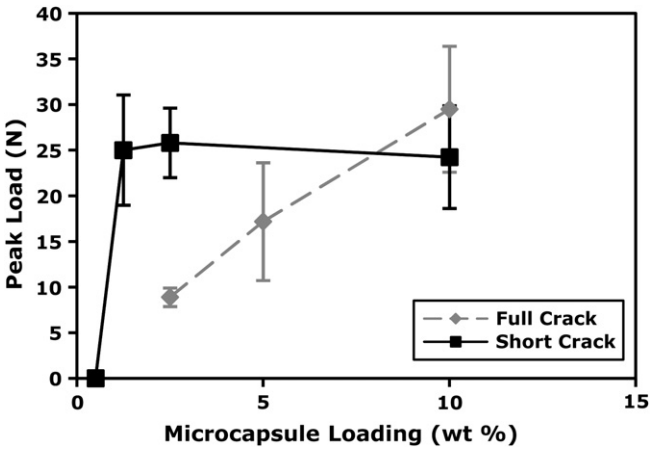

Fig. 9. Fracture test results for self-healed TDCB specimens with two different crack sizes. The microcapsules have a weight-average diameter of 251 μm and the samples contain 5 wt% of wax microspheres with embedded Grubbs' catalyst.

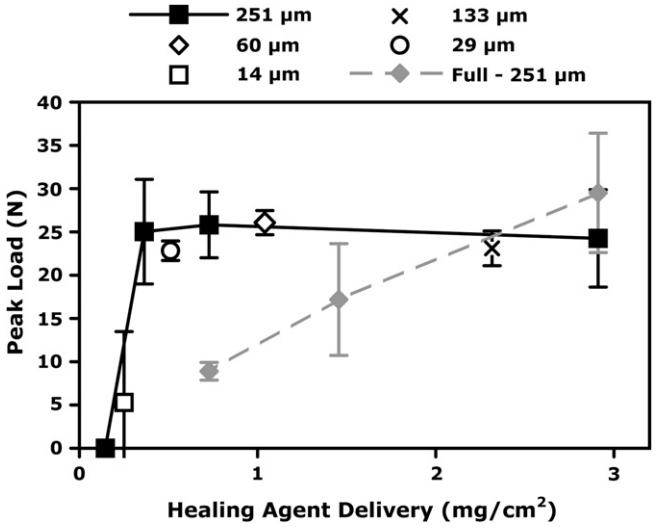

Fig. 10. Fracture test results as a function of healing agent delivery (calculated by Eq. (5)) of self-healed TDCB specimens with a short groove. Various weight fractions of 251 µm capsules are compared with 15 wt% weight fractions of various size microcapsules. For reference, the results with fully-cracked TDCB specimens with 251 µm capsules are included as well.

and given that the short-groove specimens require less healing agent, self-healing with smaller microcapsules should be possible in this case. To confirm this hypothesis, trials were also performed over a range of microcapsule size while fixing the microcapsules weight fraction at 15 wt%. (Fig. 10). The required healing agent delivery for the short-groove system is again consistent with the crack volume. With a crack separation of 3 µm, the short-groove specimen has a crack volume of about 0.3 µL/cm^2 of crack face. Thus, the minimum amount of healing agent delivery expected to fill this crack is about 0.3 mg/cm^2, which correlates well with the experimental data (Fig. 10). The maximum amount of self-healing for specimens with a 29 µm average microcapsule diameter was nearly the same as for specimens with larger microcapsules. The excellent self-healing achieved with these relatively small microcapsules is noteworthy considering that our previous reports (all with larger crack volumes) show losses in self-healing performance with microcapsules smaller than 180 µm. These data confirm that the minimum size of microcapsules needed for self-healing depends on the size of the crack that is being healed. The data also represent the most effective self-healing with the smallest microcapsules reported to date.

5. Conclusion

The amount of healing agent delivered in a self-healing material is determined by the product of the microcapsule weight fraction and the microcapsule diameter. Autonomic delivery of healing agent using microcapsules gives the same healing performance as when a similar amount of healing agent is delivered manually. If sufficient healing agent is delivered to fill the crack volume, the healing performance is maximized. However, when the crack volume exceeds the amount of available healing agent, less successful healing is achieved. When crack volumes are small (as with a crack separation of only 3 µm) self-healing can be achieved with as little as 1.25 wt% microcapsules or with microcapsules that are smaller than 30 µm. By establishing the relationship between microcapsule size, microcapsules weight fraction, and crack volume, it is now possible to rationally design self-healing systems that are tailored to repair specific types of damage.

Appendix. Fracture of TDCB specimens with localized incorporation of catalyst

Because Grubbs' catalyst is available only in limited quantities and is expensive, testing methods that minimize catalyst consumption are necessary for repetitive testing of self-healing samples and large sets of data. In these fracture tests, catalyst only participates in self-healing upon exposure on the newly fractured crack plane. Catalyst that is distant from the exposed crack plane remains unused and is wasted in self-healing evaluations. To more efficiently use the catalyst in our experimental testing program, a new specimen configuration was developed such that the catalyst phase is confined only to the regions where the damage is expected to occur, i.e. near the centerline groove in a TDCB specimen (Fig. A1). During sample fabrication, a silicone spacer is placed in the region within the mold where the catalyst-containing resin will ultimately be located. The remainder of the mold is then filled with resin to produce a "blank" that does not contain the catalyst. After a prescribed amount of cure time, the spacer is removed and this region is then filled with the catalyst-containing resin. The complete specimen is then cured for 24 h at RT followed by 24 h at 35 °C.

These "localized" TDCB specimens contain two slightly different resin formulations, one for the localized self-healing region along the centerline groove and one for the blank surrounding this region, yet they are intended to act as models for "full" specimens that have only one type of resin. We hoped to confirm whether the fracture properties of these two types of specimens are approximately equivalent. A systematic study was undertaken to compare the fracture behavior of localized TDCB and full TDCB specimens in order to demonstrate their equivalence in terms of healing assessment.

As a baseline for comparison, full TDCB specimens of EPON 828/DETA were tested yielding an average fracture toughness of 0.87 MPa m$^{1/2}$. The toughness reported here is higher than in some of our previous studies due to a slightly higher post-cure temperature used here (35 °C vs. 30 °C). Equivalent localized TDCB samples were then prepared with neat resin in both the blank and center regions. The average fracture toughness of these specimens is only slightly higher than with the full TDCB geometry (Table A1). When 5 wt% of catalyst-containing wax microspheres are included in the center region, the average fracture toughness is equivalent to that obtained for the full TDCB of neat epoxy (Table A1).

When 10 wt% of capsules were added to full TDCB specimens, the fracture toughness increases to 0.98 MPa m$^{1/2}$ (Table A2). The increase in toughness due to the addition of

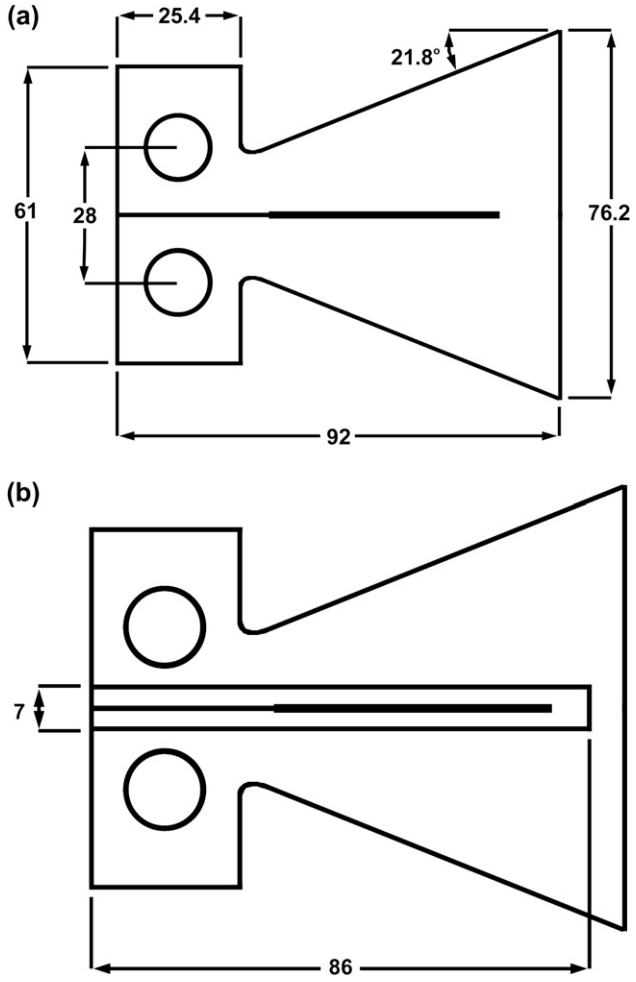

Fig. A1. Schematic drawings of (a) full TDCB specimen and (b) localized TDCB specimen in which the resin formulation in the center section may be different from that in the rest of the specimen.

microcapsules has been reported previously [11]. However, for localized specimens with neat resin in the blank and 10 wt% microcapsules in the center region, the average fracture toughness increases to 1.38 MPa $m^{1/2}$. This 40% increase in fracture toughness is likely due to increased residual stresses resulting from the difference in properties between the neat resin in the blank and the resin with microcapsules in the center region.

To avoid this mismatch, samples were prepared with microcapsules in both the blank and the center region. When this type of blank is cured for 24 h before filling the center section, the fracture toughness is much closer to that of the full TDCB specimens (Table A2). Similarly, when the blank is cured for only 3 h before being filled, the average fracture toughness is even closer. Thus, when microcapsules are present in both the blank and the center region, the localized samples have similar fracture properties compared to full TDCB specimens.

As a final confirmation, samples were prepared with 10 wt% capsules in the blank and 10 wt% capsules and 5 wt% wax-protected catalyst in the center region. These specimens have an average fracture toughness that is only slightly higher than full TDCB specimens with 10 wt% microcapsules (Table A2).

Overall, localized TDCB specimens greatly reduce the amount of catalyst required while providing a reasonable approximation of the fracture properties of full TDCB specimens when a similar weight fraction of microcapsules is used in both the blank and the center regions. Similarly, it appears that the presence of wax-protected catalyst in the center region (but not in the blank) has relatively little influence on the fracture properties.

The TDCB specimen with a short groove (which is used to produce less crack face separation) is similar to the localized TDCB described above, but the groove is shortened from 47 mm to 25 mm (Fig. A1). In addition, the center section which contains the catalyst has a total length of 64 mm rather than 86 mm. In all other dimensions, it is identical to the TDCB specimens used in our previous self-healing trials.

Table A1
TDCB fracture results without microcapsules

Sample type	Catalyst[a] (wt%)	No. of samples	K_{IC}[b] (MPa $m^{1/2}$)
Full	0	13	0.87 ± 0.12
Localized	0	6	0.96 ± 0.09
Localized	5	60	0.88 ± 0.10

[a] Weight fraction of wax microspheres containing 5 wt% Grubbs' catalyst included only in the sample's center section.
[b] Average values $\pm$ 1 standard deviation.

Table A2
TDCB fracture results with 10 wt% microcapsules[a]

Sample type	Microcapsules in blank[b] (wt%)	Blank cure time[c] (h)	Catalyst[d] (wt%)	No. of samples	K_{IC}[e] (MPa $m^{1/2}$)
Full	na	na	0	17	0.98 ± 0.12
Localized	0	24	0	5	1.38 ± 0.10
Localized	10	24	0	11	1.06 ± 0.16
Localized	10	3	0	4	1.03 ± 0.10
Localized	10	3	5	30	1.08 ± 0.15

[a] All samples contain 10 wt% of DCPD-filled microcapsules in either the entire sample (full) or in the sample's center section (localized).
[b] Microcapsule weight fraction in the sample's exterior section.
[c] Cure time for sample's exterior section before adding the resin for the center section.
[d] Weight fraction of wax microspheres containing 5 wt% Grubbs' catalyst included in the center section.
[e] Average values $\pm$ 1 standard deviation.

References

[1] Lendlein A, Kelch S. Angewandte Chemie International Edition 2002; 41(12):2034.
[2] Luzinov I, Minko S, Tsukruk VV. Progress in Polymer Science 2004;29(7):635.
[3] White SR, Sottos NR, Geubelle PH, Moore JS, Kessler MR, Sriram SR, et al. Nature 2001;409(6822):794.
[4] Chen XX, Dam MA, Ono K, Mal A, Shen HB, Nutt SR, et al. Science 2002;295(5560):1698.
[5] Chen XX, Wudl F, Mal AK, Shen HB, Nutt SR. Macromolecules 2003;36(6):1802.
[6] Pang JWC, Bond IP. Composites Science and Technology 2005;65 (11–12):1791.
[7] Lee JY, Buxton GA, Balazs AC. Journal of Chemical Physics 2004; 121(11):5531.

[8] Brown EN, Sottos NR, White SR. Experimental Mechanics 2002; 42(4):372.
[9] Brown EN, Kessler MR, Sottos NR, White SR. Journal of Microencapsulation 2003;20(6):719.
[10] Kessler MR, Sottos NR, White SR. Composites Part A Applied Science and Manufacturing 2003;34(8):743.
[11] Brown EN, White SR, Sottos NR. Journal of Materials Science 2004;39:1703.
[12] Rule JD, Brown EN, Sottos NR, White SR, Moore JS. Advanced Materials 2005;17(2):205.
[13] Brown EN, White SR, Sottos NR. Composites Science and Technology 2005;65(15–16):2466.
[14] Brown EN, White SR, Sottos NR. Composites Science and Technology 2005;65(15–16):2474.
[15] Cho SH, Andersson HM, White SR, Sottos NR, Braun PV. Advanced Materials 2006;18(8):997.
[16] Landfester K. Advanced Materials 2001;13(10):765.
[17] Schork FJ, Luo Y, Smulders W, Russum JP, Butte A, Fontenot K. Advances in Polymer Science 2005;175:129.
[18] Asua JM. Progress in Polymer Science 2002;27:1283.
[19] Loscertales IG, Barrero A, Guerroro I, Cortijo R, Marquez M, Ganan-Calvo AM. Science 2002;295:1695.
[20] Ma GH, Su ZG, Omi S, Sundberg D, Stubbs J. Journal of Colloid and Interface Science 2003;266:282.
[21] Schwab P, Grubbs RH, Ziller JW. Journal of the American Chemical Society 1996;118(1):100.
[22] Jones AS, Rule JD, Moore JS, White SR, Sottos NR. Chemistry of Materials 2006;18(5):1312.